5-2016

Thermoluminescence study of Mn doped lithium tetraborate powder and pellet samples synthesized by solution combustion synthesis

A. Özdemir
Çukurova University

Zehra Yeğingil
Çukurova University

Necmettin Nur
Adiyaman University

Kasim Kurt
Mersin University

Tunç Tüken
Çukurova University

See next page for additional authors

Thermoluminescence study of Mn doped lithium tetraborate powder and pellet samples synthesized by Solution Combustion Synthesis

A. Ozdemir[1], Z. Yegingil[1], N. Nur[2*], K. Kurt[3], T. Tuken[4], T. Depci[5], G. Tansug[6], V. Altunal[1], V. Guckan[1], G. Sigircik[4], Y. Yu[7], M. Karatasli[1], Y. Dölek[8]

[1]*Çukurova University, Art Sciences Faculty, Physics Department 01330 Balcalı Sarıçam Adana TURKEY*
[2]*Adiyaman University, Engineering Faculty, Department of Electrical Electronic Engineering 02040 Adiyaman TURKEY*
[3]*Mersin University, Art Sciences Faculty, Physics Department Mersin TURKEY*
[4]*Çukurova University, Art Sciences Faculty, Chemistry Department 01330 Balcalı, Sarıçam, Adana TURKEY*
[5]*Inonu University, Engineering Faculty, Department of Mining Engineering, 44280 Malatya TURKEY*
[6]*Çukurova University, Ceyhan Engineering Faculty, Department of Chemical Engineering, Adana TURKEY*
[7]*Sidney Kimmel Medical College at Thomas Jefferson University, Philadelphia, PA USA*
[8]*Baskent University Hospital, Barracks Health Campus, Radiation Oncology Department, Adana TURKEY*

Abstract

In this paper, the thermoluminescence (TL) dosimetric characteristics under beta-ray, x-ray and gamma-ray excitations of powder and pellet Mn-doped lithium tetraborates (LTB) which were produced by solution combustion synthesis technique were investigated, and the results were compared with that of TLD-100 chips. The chemical composition and morphologies of the obtained LTB and Mn-doped LTB (LTB:Mn) were confirmed by an X-ray diffraction (XRD), Fourier Transform Infrared (FTIR) and scanning electron microscopy (SEM) with EDX. LTB:Mn was studied using luminescence spectroscopy. In addition, the effects of sintering and annealing temperatures and times on the thermoluminescence (TL) properties of LTB:Mn were investigated. The glow curves of powder samples as well as pellet samples exposed to different beta doses exhibited a low temperature peak at about 100 °C followed by an intense principal high temperature peak at about 260 °C. The kinetic parameters (E, b, s) associated with the prominent glow peaks were estimated using T_m-T_{stop}, initial rise (IR) and computerized glow curve deconvolution (CGCD) methods. The TL response of integral TL output increased linearly with increasing the dose in the range of 0.1 - 10 Gy and was followed by a superlinearity up to 100 Gy both for powder and pellet samples using beta-rays. Powder and pellet LTB:Mn were irradiated to a known dose by a linear accelerator with 6 and 18 MV photon beams, 6 to 15 MeV electron beams and a traceable ^{137}Cs beam to investigate energy response. Further, TL sensitivity, fading properties and recycling effects related with beta exposure of LTB:Mn phosphor were evaluated and its relative energy response was also compared with that of TLD100 chips. The comparison of the results showed that the obtained phosphors have good TL dose response with adequate sensitivity and linearity for the measurement of medical doses.

Keywords: Manganese doped $Li_2B_4O_7$; Solution Combustion Synthesis method; Dose response; Energy response; $T_m - T_{stop}$; IR; CGCD

* Corresponding author. Tel.: +90 416 223 38 00/2867
E-mail address: nnur@adiyaman.edu.tr (N. Nur).

1. Introduction

The tissue equivalent thermoluminescence materials are very suitable in clinical applications such as radiological examinations and therapeutic treatments. Lithium tetraborate is a promising material for dosimetric application, and well-documented lithium borate compound has an effective atomic number of Z_{eff} =7.3, which is very close to the soft biological tissue (Z_{eff} =7.4). The number of the phosphors with this effective atomic number is not high for the determination of the absorbed dose in soft tissue. Great attention has been devoted to the synthesis and characterization of both pure LTB and transition elements and rare earth elements doped LTB. The aim since the 1960s has been the understanding of the sintering process, the evolution of microstructure development, and identifying and manufacturing new LTB phosphors for dosimetric purposes [1,2,3,4,5,6,7,8,9,10,11]. Particularly, the main dosimetric characteristics of doped lithium tetraborate phosphors, LTB:Cu,In,Ag and LTB:Cu,In [12], LTB:Cu,In and LTB:Cu [13], LTB:Mn and LTB:Ag [14] have been reported. Kaczmarek studied the effect of various impurities (Cr, Co, Eu, Dy) in LTB glasses melted in oxygen and hydrogen on the absorption and emission spectra for valency state analysis [15]. Kaczmarek et al., have measured the absorption and emission spectra of LTB:Eu,Dy, LTB:Yb, LTB:Ti glasses; the authors observed possible energy transfer from Eu^{2+} to Dy^{3+} ions [16]. Piwowarska et al., have carried out a study of the electron paramagnetic resonance (EPR) and optical absorption spectra of LTB single crystals doped with Co^{2+} ions. The EPR data revealed at least two types of Co^{2+} centers and confirmed octahedral coordination of Co^{2+} ions and cation vacancies arising in the ''as-grown'' crystal [17]. In 2011, Pekpak et al., synthesized LTB by two different synthesis methods—high temperature solid state synthesis and water/solution assisted synthesis—and doped different amounts of Cu, Ag and In into the main matrix. They investigated the effect of synthesis methods and dopant amount and type on TL glow curve structure [18]. LTB was synthesized by the solid state method and Cu, Ag, P, In and Mn and their combination were doped into the LTB by Annalakshmi et al. They have carried out an extensive study of the glow curve structure and kinetics of the obtained phosphors [19].

Particularly, Mn as a dopant has been evaluated for LTB matrix and LTB:Mn phosphor has been systematically explored for thermoluminescence dosimetry. LTB was activated with 0.1 wt. % Mn by Schulman et al., and the results showed that its sensitivity was 10 times lower than LiF (TLD100) and was described as being caused by the emission, which is out of the response range of the photomultipliers [1]. Podgórska et al., in a series of papers over the past ten years, have studied transition metal ions (Mn, Co, Cr, Ti) doped to LTB single crystals and glasses. Single crysyals of LTB doped with Mn^{2+} (0.014 mol. %) and LTB glasses doped with Mn^{2+} (0.1 mol. %) have been demonstrated using the EPR method. In both systems the Mn ion is found to enter substantially for the Li^{+} ion as Mn^{2+} and/or Mn^{1+}, and probably for the B^{3+} ion or interstitial as Mn^{3+} [20]. They have further investigated the growth conditions of LTB single crystals in both pure and Yb, Co, Mn doped systems. The crystals were grown by the Czochralski method using the concentration of the Yb, Co, Mn ions at a level of 0.5 mol. %. Some thermoluminescence properties, like energies and lifetimes of the traps of different charge carriers occurring in the crystal at low temperatures, were measured [21]. Recently, Kayhan and Yilmaz synthesized LTB by different synthesis methods and various amounts of Mn were doped into the LTB alone and with different co-dopants, Ag, P and Mg. They declared that Mn is an efficient dopant for the LTB matrix [22]. In the same year, Mn was doped into LTB by Annalakshmi et al., who determined the optimum Mn concentration to be obtained the optimal TL intensity. They found the high temperature peak of the TL glow curve at 250 ^{0}C, which is higher

than the temperature obtained in the literature, and the neutron dose response was found to be 25% of that of TLD-600 [9]. Electron paramagnetic resonance parameters and luminescence properties of LTB:Mn, LTB:Mn, Be and LTB:Mn, Cu were studied by Nagirnyi et al., who suggested that LTB:Mn showed good TL response, Cu as a co-dopant increase the sensitivity, and the TL peak obtained at 490 K is related with the hole mobility [23]. Drozdowski et al., studied LTB single crystals doped with Mn and Eu. The glow curves have been recorded between 10 and 300 K in order to focus attention on shallow traps. A broad, intense glow peak is observed around 80 K, with three weaker peaks at 205, 255, and 280 K [24]. Kar et al. irradiated undoped and Mn and Cu doped single crystal, polycrystalline and glass LTB by X-rays. They obtained two well-separated main peaks in TL glow curves belonging to single and polycrystalline LTB:Mn, whereas the glass form of LTB indicated one peak and the doping procedure increased the TL efficiency [25]. Annalakshmi et al., prepared LTB:Mn by solid state sintering method and its main TL properties were investigated. The maximum TL peak was observed at 280°C and no fading was recorded for three months. The sensitivity was determined as 0.9 times lower than that of TLD-100 [26].

In addition, LTB compounds are traditionally studied as efficient materials for nonlinear optics, acoustic electronics, and piezo-technology and have been used in various areas of science and industry with increasing demand. One of the most important characteristics of thermoluminescent LTB is its high thermal neutron cross section. ^{6}Li and ^{7}Li isotopes of lithium have the same response for the fast neutrons and gamma-rays of a mixed radiation field which contains, besides these two, also thermal neutrons. NIST (National Institute of Standards and Technology) reported a higher thermal neutron cross section for ^{6}Li [27]. $Li_2B_4O_7$, if it is developed to employ the isotopes of ^{6}Li and ^{10}B with a large capture cross-section value for thermal neutrons, has an additional advantage of neutron detection due to charged particle production reactions [9,28,29].

In this work, LTB:Mn (0.04 M %) microstructured phosphor was synthesized by the solution combustion synthesis technique. The morphology, structure and chemical composition were determined by X-ray diffraction (XRD), Fourier Transform Infrared (FTIR) and scanning electron microscopy (SEM) with EDX. The emission of Mn^{2+} centers is observed in the photoluminescence spectra. LTB:Mn was investigated by thermoluminescence under beta-ray, x-ray and gamma-ray excitations. The numbers of peaks within the relevant regions of the glow curve, an estimate of the activation energy E and the frequency factor *'s'* as well as *'b',* were achieved by the T_m-T_{stop} , initial rise (IR) and computerized glow curve deconvolution (CGCD) methods. The main dosimetric properties, annealing procedure, TL sensitivity, beta-ray dose response, relative photon and electron energy response, reproducibility and fading at storage of LTB:Mn were also investigated.

2. Materials and Methods

2.1 Material synthesis

In this study, Mn activated LTB phosphor was prepared by Solution Combustion Synthesis (SCS) method. The experimental procedure for preparing crystallites by the SCS method consisted of mixing stoichiometric amounts of starting materials lithium nitrate $LiNO_3$ with the boric acid H_3BO_3 and then adding dopant of manganese nitrate $Mn(NO_3)_2$ to the mixture. Urea (CH_4N_2O) as fuel was also added to this mixture. After the formation of precipitation and imparting white/grayish body color, the prepared phosphor LTB:Mn was ground into a fine powder using agate mortar, transferred to the

platinum crucible, and heated in a furnace with a heating rate of 5 ^{0}C/min from room temperature to various predetermined temperatures of 600, 700, 800, 825, 850 and 875 ^{0}C for one hour. The higher temperatures of 825, 850 and 875 ^{0}C led the precipitation to be melted into a homogeneous mixture in our experiments. It was deduced that 800 ^{0}C is the maximum temperature for sintering of LTB:Mn. To check the relation between sintering temperature and TL efficiency, the LTB:Mn powder samples sintered for different temperatures of 600, 700 and 800 ^{0}C for retention time of 1 hour were read out after 1 Gy beta irradiation (see Fig. 1). They exhibited the highest TL sensitivity for 800^0 C sintering temperature.

The effect of sintering time on the microstructured phosphor was also determined. We increased the sintering time beginning at 30 minutes to 1, 1.5, 2, 2.5 hours at the sintering temperature of 800 ^{0}C. The effect of sintering time on TL measurements was achieved by comparing the TL glow curves after exposing the phosphors sintered at different times to 1 Gy beta irradiation. The increasing time had a significant effect on the peak heights of the glow curves. The maximum termoluminescence responses were observed when they were sintered for 30 minutes and 2.5 hours. It is demonstrated in Fig 2. In this study, we chose 30 minutes as the sintering time of the LTB:Mn specimens.

In this study, the cooling rate employed was furnace cooling with power off. The samples inside the furnace were allowed to cool back down to 25 ^{0}C. They appeared highly hygroscopic and were grounded in a mortar. Then, they were kept at 70 ^{0}C in a drying oven. In order to minimize the amount of absorbed water, to solidify the LTB:Mn TL material and to handle the samples easily, the binder component KBr in the weight ratio 1:1 was mixed with the main phosphor matrix. After the mixing step, the mixture was molded under pressure using a die and formed the TLD pellets (6.0 mm diameter and 0.5 mm thickness). For their microscopic structure not to be deformed the molded bodies were sintered at 400 for 30 minutes.

2.2 Material characterization techniques

We studied LTB:Mn material structure of the eventual products to be sure that the productions have been presenting the intended samples. The Rigaku, SmartLab x-ray Diffractometer (XRD) Cu-Kα (λ=1.5406A^o) was used for the structural analysis. Surface morphological analysis was recorded on scanning electron microscope (FE-SEM with EDX), Zeiss, Supra 55 with a spectral slit width of 1.5 nm at room temperature. A Fourier transform infrared (FT-IR) spectroscopy, Thermo Scientific, Nicolet iS10, equipped with the Universal ATR sampling accessory was used to determine the vibrational bonds in the 4000-550 cm^{-1} region.

The photoluminescence (PL) and photoluminescence excitation (PLE) spectra were measured using a Horiba/Jobin-Yvon Fluorolog-3 spectrofluorometer with a 450 W xenon lamp and a Hamamatsu R928P photomultiplier. The PLE spectra were corrected by the xenon lamp emission spectrum. The PL spectra were corrected by the photomultiplier spectral response.

2.3 Thermoluminescence measurements

The TL glow curves of the synthesized LTB:Mn were obtained using a RISO TL/OSL reader model DA-20. Beta irradiation at room temperature was done using a ^{90}Sr/^{90}Y source with a dose rate 6.689 Gy/min mounted within the TL equipment. For each measurement, an approximately 7 mg of phosphor

was taken and put into planchet uniformly. The normal readout of the powder and pellet samples included heating them with a constant heating rate of 2 ^{0}C/s from room temperature up to 450 ^{0}C. Due to the shallow traps tend to fade more rapidly at normal ambient temperatures than do the deep traps, we did preheating and heated samples up to 160 ^{0}C for 10 s before TL read out to minimize the population of the low level traps, in our measurements.

In this study, the TL sensitivity is expressed as both the glow curve area and/or peak height per unit mass of the dosimeter. The kinetic parameters of the phosphor were obtained using different methods: T_m-T_{stop} method, initial rise (IR) method and computerized glow curve deconvolution method (CGCD).

For the dosimetric characterization of the LTB:Mn TL material, the dose response over the dose range of 0.1 – 100 Gy of beta radiation (^{90}Sr/^{90}Y) and the variation of response with photon and/or electron energies were studied. Irradiation of the thermoluminescent $Li_2B_4O_7$:Mn to two different values of x-ray energies of 6 MV and 18 MV besides the electron energies of 6, 9, 12 and 15 MeV using the therapy radiation beam Varian DHX SN3323 LINAC was performed at Baskent University Hospital, Radiation Oncology Department in Adana, Turkey. This medical LINAC is calibrated in terms of the protocol of the International Atomic Energy Agency (IAEA 1987) using a calibrated Paralel-plate Roos ionization chamber (PWT 34001). The calibration factor is traceable to the Turkish Atomic Energy Agency (TAEK). Low energy gamma irradiation was carried out using a ^{137}Cs irradiator obtained from GAMMACELL 3000 ELAN containing a Cs^{137} source, traceable to the Turkish Atomic Energy Agency (TAEK), with a dose rate of External Dose Rate: ≤ 5 μSv/h (0.5 mrem/h) at 5 cm (1.94 in) from front and Central Dose Rate: 4.5 or 8.7 Gy/min (± 20%) at Baskent University Hospital, the Transfusion Center in Adana, Turkey. The low energy x-ray exposure was achieved from a 220 kV_p x-ray tube established in a Small Animal Cone Beam CT Guided X-Irradiation System (SARRP), in the energy range 40-80 keV with 13mA, broad focus and Cu filter at Thomas Jefferson University, Sidney Kimmel Medical College, Philadelphia, USA.

3. Results and Discussion

3.1 Characterization of Lithium Tetraborate

The characterization of undoped and doped lithium tetraborate synthesized by solution combustion method were evaluated by XRD, FTIR and SEM with EDX. Analysis of XRD patterns and band positions of IR spectra of synthesized materials showed that the best sintering temperature and time have been found as 800 °C and 30 minutes. No peaks or IR bands were observed associated with dopant (0.04 % mol Mn) in patterns or in the spectra. XRD pattern, IR spectrum and SEM images of LTB:Mn are given in Fig 3.

Analysis of the powder X-ray diffraction data of $Li_2B_4O_7$ (Fig. 3a) proved that all of the reflections matched with the powder diffraction data of $Li_2B_4O_7$ reported in JCPDS Card No: 18-0717 and neither pronounced distortions nor separate phases in the XRD pattern were detected depending on the dopant because of too low concentration. Besides this, the cell parameters and indexing were analyzed and found using the least square procedure employing a locally modified version of the program CELLREFF [30]. The unit cell parameters were calculated as follows: a=b=9.462 A$^\circ$ and c=10.271 A$^\circ$, which are close to the JCPDS Card No: 18-0717, in which a=b=9.4771 A$^\circ$, and c= 10.286 A$^\circ$.

IR spectrum of $Li_2B_4O_7$ is given in Fig. 3b. Approximately 14 clear bands were recorded in the region 400–2000 cm^{-1}. The peaks are at 1382, 1344 and 1315 cm^{-1} related with the B-O stretching trigonal BO_3 units 1131, 951, 868 and 804 cm^{-1} showing the B-O stretching of tetrahedral BO_4^- units and the others bending vibrations of various borate segments. No difference has been observed on the IR spectrum, meaning that the structure of lithium tetraborate did not change and no new borate compounds occurred with added Mn.

SEM micrographs of Mn-doped $Li_2B_4O_7$ are given in Fig. 3c and 3d, indicating the porous structure, agglomerated particles and spherical type morphology. The literature survey show that this type morphology is generally seen due to evolved gases during the combustion synthesized oxide phosphors [31,32,33]. The particle size was found to be between 882.7 nm and 1.546 μm. The Mn concentration in mol was confirmed as 0.04 % using EDX.

PL and PLE spectra of the studied samples are presented in Fig. 4 and Fig. 5, respectively. As it is evident from the figures, the emission spectrum at photoexcitation represents a single broad band peaked at about 600 nm. The characteristic excitation spectrum with main line peaked at 409 nm testify unambiguously the Mn^{2+} ions responsible for this emission [14].

3.2 Thermoluminescence characteristics of lithium borates

3.2.1 TL Glow Curves

The powder and pellet LTB:Mn samples were exposed to a 2 Gy beta dose and were then read out. Every data point in the obtained results was acquired by the measurements of three planchets. The typical glow curves are given in Fig. 6. Both the powder and pellet LTB:Mn samples demonstrate two groups of TL maxima. The first one, a low temperature peak at around 100 ^{0}C decays very soon after exposure and warrants further discussion in a later section. Hence, it was estimated to not be a dosimetric peak. The high temperature peaks located below 300 ^{0}C and above 200 ^{0}C merged into a single peak. The second group of TL maxima with an intense high temperature peak at about 260 ^{0}C was used in TL emission determinations in our measurements. The same TL peaks have been reported before in various literature [34,9,19].

3.2.2 Evaluating the trapping parameters

After irradiation of the phosphors, at constant temperature, thermoluminescence intensity I(T) is defined as the rate of decrease of the number of trapped electrons and given by the equation

$$I(T) = - dn/dt = n^b s' \exp[-E/kT] \qquad (1)$$

where n is the number of trapped charges at the trap depth (activation energy) E [eV] at a time t and absolute temperature T (K); b the order of kinetics ($1 < b \leq 2$); s' [$s(s^{-1})$] the frequency factor of the trap and is related to the lattice phonon vibrational frequency and the entropy change associated with the transition; k [eV K^{-1}] the Boltzman constant [35].

In order to extract information from the thermoluminescence signal it is necessary to assume suitable models for the possible processes: (1) Randall and Wilkins model: It leads the first order description of the TL process and suggests one type trap and one type recombination (s'=s and b = 1). (2) Garlick and Gibson model: It leads to the second order TL process (s' = s/N, where N is the whole concentration of the charge traps and b = 2). (3) The glow peak shape does not obey the rules of the first or second order glow curves: May and Partridge suggested a general order glow curve (mixed order glow curve; 1 < b < 2) [35].

The determination of number and positions of the overlapped peaks within a glow curve was suggested by McKeever using a technique called the T_m–T_{Stop} [36]. In this method, the sample is irradiated and the TL curve is erased up to a temperature T_{Stop} by partially heating the sample. Then the sample is cooled down to room temperature and re-heated for recording the remaining curve. The first maximum T_m of the glow curve is determined for each TL reading. T_m versus T_{Stop} plot is made and the probable positions of the main TL peaks are decided. This plot can exhibit a straight line with zero slope or a characteristic "staircase" shape. In the former, the peak is simple first order; in the latter, each flat region in the curve corresponds to an individual first order peak. If the T_m–T_{Stop} curve has the shape of a curved line, a smooth staircase curve, it shows second order peaks. The kinetic parameters can be obtained using a curve fitting procedure [35,37].

It was one of the purposes of this study to investigate the kinetic parameters (E, s and b) accompanying with the TL glow curves of powder LTB:Mn phosphor samples. The depths and other properties of electron or hole traps were deduced using the glow curves which were estimated as composed of several peaks that lie partly over each other. For this purpose, each individual TL peak was isolated using the T_m-T_{stop} method. In addition to this method we made the glow curve analysis using deconvolution, which is widely applicable for computing peak temperatures of distinguished peaks. Once the kinetic order b and number of isolated TL glow peaks in a composite TL glow curve are known E and s values can be investigated [6,38]. Accordingly, in this study, we first used the T_m-T_{stop} method to separate the composite TL glow curve into its component peaks using the T_m-T_{stop} curve and estimate the number of peaks. Then, b was determined from the shape of the flat regions of the same T_m-T_{stop} curve. In this process, the annealing procedure at 400 ^{0}C for 30 minutes was carried out for each single fresh powder sample, each time. The irradiations of the samples with a 5 Gy dose prior to the TL measurements were carried out using the ^{90}Sr/^{90}Y beta-rays source of the Riso TL machine. The TL glow curves were acquired 6 hours after the exposure to beta-rays. TL measurements were done from 160 ^{0}C up to 450 ^{0}C and the kinetics data was examined just for the high temperature (~ 260 ^{0}C) peak of LTB:Mn specimens. Linear heating rate 2 ^{0}C/s was employed. The process was repeated on freshly irradiated samples using different values of T_{stop} each time, increasing T_{stop} 2 ^{0}C each time and the T_m values were recorded again.

In this study, we plotted T_m versus T_{stop} for the LTB:Mn phosphors exposed to a 5 Gy beta dose (see Fig. 7). The important features estimated from this graph are: The flat regions in the T_m-T_{stop} curve represent individual peaks which are not apparent in the original glow curve. There are three separated TL peaks in the temperature region examined: one at about 220 ^{0}C, the second at 268 ^{0}C and the third around 292 ^{0}C. However, it can be clearly seen in the regions of peaks that there is no clear plateau but rather a slight increase at the first stage and then a quick increase at the end. The rise of T_m with an incline at the end of the narrow flat region indicates that the order of glow peaks is higher than first order (see Fig. 7). Thus, the TL peaks under the glow curve are at 220 ^{0}C, 268 ^{0}C

and 292 ^{0}C follow mixed order kinetics (1<b<2) because of an incline at the end of the flat region for each T_m.

Analysis of thermoluminescence composite curves was also carried out by the IR method after T_m -T_{stop} measurements. This method suggests that the initial part of the TL glow curve is an exponential function of the temperature as given in Eq. (2), and is independent of the order of kinetics [39,40]. The initial region of the TL signals up to ~10% of its peak maximum (I_m) were evaluated using this method. A plot of ln(I) versus 1/T gave a smooth line with a slope of –E/kT; from that a series of activation energies E was calculated.

$$I(T) \propto \exp[-E/kT] \qquad (2)$$

The obtained values of the activation energy for each heating-cooling process in the T_m-T_{stop} measurements are given in Fig. 8, showing three groups of activation energies. It can be established confirming that three TL peaks are seen in that temperature range. Thus, IR method determines at least three peaks in that temperature range from 160 ^{0}C to 300 ^{0}C. The first plateau region is between 176 ^{0}C and 184 ^{0}C, which is nearly constant around 1.03 ± 0.12 eV. It might be connected to the peak P_1 at around 220 ^{0}C. The second plateau region is between 200 ^{0}C and 210 ^{0}C, which is at about 1.22± 0.05 eV. This flat region is correlated with the peak P_2 at around 268 ^{0}C. The third flat region is appearing between 232 ^{0}C and 246 ^{0}C, which is nearly constant at around 1.45± 0.04 eV. It is correlated with the peak P_3 at around 292 ^{0}C. The values of activation energies (from Fig. 8) are given in Table 1.

The T_m-T_{stop} method, along with IR method, is pretty powerful to obtain component glow peaks of the composite glow curves and activation energies of each component glow peak [40]. In the present study, the computerized glow curve deconvolution (CGCD) method was also used to analyze all the glow curves. The application of CGCD technique for separation of composite TL glow curve into its individual glow peaks is widely exerted for decays [4]. The kinetic parameters E, s and b, evaluated by deconvolution method, highly depend upon input parameters used in the deconvolution software [40]. In this study, the CGCD analysis was performed using a script software for mixed order kinetic equations, which uses Kitis equations [41], by adapting it to *the program of origin* for the deconvolution of the TL glow curves of LTB:Mn. The input parameters and the peak locations, derived from the T_m-T_{stop} method, were used for deconvolution. Three glow peaks were deconvoluted to obtain an exact fit with experimental TL glow curves by the CGCD method (see Fig. 9). Activation energies (E) were also calculated after the determination of the peak temperatures by the CGCD method. The kinetic orders and frequency factors were obtained by the curve fitting procedure of matching the computer software generated curve with TL glow curve. All TL kinetic parameters determined are shown in Table 1. As seen from Table 1, kinetic parameter values of the evaluated three glow peaks, P_1, P_2 and P_3 determined by IR and CGCD methods follow values within the error range.

3.3 Pre-irradiation annealing procedures

TL technique requires repeating the procedures of preheating and annealing. Accepted procedures for annealing the TLDs in many cases not only eliminate all of the stored energy trapped in the crystal lattice during the high level exposures but also restore the original sensitivity [35].

In this study, we examined various heat treatments for routine handling of our specimens. In our measurements on determination of annealing temperature and time, all of the materials were in the form of powder samples. A group of samples were exposed to a 2 Gy dose of beta irradiation after an anneal procedure of 30 minutes at 300, 350, and 400 ^{0}C. The dosimeters yielded a high peak amplitude at 400 ^{0}C. To be sure that all of the stored energy trapped in the crystal lattice during the high level of radiation is eliminated we exposed the samples to a 100 Gy beta dose. The samples were annealed for 15, 30 and 45 minutes at various degrees of temperature, 300, 350 and 400 ^{0}C. The anneal procedure of 400 ^{0}C for 30 minutes emptied the trapped electrons and was determined as annealing conditions for this study.

3.4 Dose response

In this study, the dose response curves which show the relationship between the TL intensity and changes in the dose of LTB:Mn polycrystalline phosphor in stoichiometric compositions were determined. The integrated TL glow curve area for the powder and pellet samples plotted against varying doses from 0.1 Gy to 100 Gy (0.1, 0.2, 0.5, 1.0, 2.0, 5.0, 10.0, 20.0, 50.0 and 100.0 Gy) after beta-ray irradiation (see Fig. 10). The same process was repeated together with the TLD100 chips for the dose values 0.1 Gy to 10 Gy (0.1, 0.2, 0.5, 1.0, 2.0, 5.0 and 10.0 Gy) (see Fig. 11). TL pulses integrated over the all-dosimetric peak, only including its high temperature section from 160 ^{0}C to 450 ^{0}C, with no glow peak deconvolution, was evaluated and plotted versus the exposed dose values. They exhibited great linearity up to 10 Gy. The final dose response curves were well fitted by the straight lines with the superlinearity index g(D) = 1. Above this dose level, up to 100 Gy, superlinear dose dependence of TL with g(D) > 1 was obtained. These subsets were then compared on the basis of slope of their dose response curves. As it was expected, both powder and pellet samples yielded the same slope with g(D) > 1 and g(D) = 1 for the two group of dose response measurements, 0.1 Gy ≤ D ≤ 100 Gy and 0.1 Gy ≤ D ≤ 10 Gy, respectively (see Fig.10 an Fig.11). The powder LTB:Mn samples appeared to be more sensitive to radiation exposure than the pellet samples in TL readings.

Fig. 11 shows a comparison of the measured TL intensity (I) profile along the y-axis using beta-ray exposure for the powder and pellet LTB:Mn samples and TLD100 chips in the rather low dose region as this dose region is usually the dose operating range for TLD100 dosimeters. It was demonstrated that with increasing dose value (D), TL intensity (I) linearly increases for both of the powder and pellet LTB;Mn samples, and also for TLD100 chips. The high temperature peaks of ~ 260 ^{0}C for both LTB:Mn powder and pellet samples showed linear behavior at low dose levels (1 < D < 10 Gy) with g(D) = 1, as shown in Fig. 11. g(D) for TLD100 chips was evaluated as g(D)=~1 (see Fig. 11). We also found that in the dose range lower than 10 Gy, the differences of the dose response values of TLD100 chips and that of LTB:Mn powder and pellet samples decrease with increasing dose values. The relative sensitivity of powder LTB:Mn sample was determined as one tenth of sensitivity of TLD100 after a 10 Gy beta dose exposure. The same results in dose response studies of LTB:Mn with various concentrations of Mn have been reported in the literature [42]. Annalakshmi et al. investigated the TL properties of LTB:Mn (0.32 wt % Mn) with variable gamma exposures using Cs-137 and Co-60 sources. They found that the response of the phosphor show linearity up to 10 Gy followed by a supralinearity untill 10^3 Gy which is the saturation dose [9].

3.5 Photon energy response

The powder and pellet LTB:Mn phosphors, and TLD100 chips were irradiated with varied photon energies of 0.662 MV from ^{137}Cs, and 6 MV and 18 MV from linear accelerator and electron energies in the range of 6 to 15 MeV from linear accelerator. The energy dependence (photon and/or electron energy response) has been indicated based on the yielded data of total counts in maximum height/mg for each response to delivered photon and electron energy. After a 2 Gy dose exposure in all photon energies, for powder and pellet LTB:Mn 0.04 M % phosphors, the energy response was found to exhibit progressions in the same direction as parallel but shifting from each other, and it was found that the sensitivity of the powder samples is around six times higher than that of pellet samples for each energy value. For 0.662 MV γ-ray photon energy, the measured response of LTB:Mn 0.04 M % powder and pellet phosphors was about 17 % higher than that measured for 6 and 18 MV photon energies. The resultant deviation in the form of a slope represents a degree of energy dependence in this low energy range. The ratio of 0.662 MV photons to 6 and/or 18 MV photons responses quantifies this factor. There was not an appreciable difference in the response for 6 and 18 MV photons for individual energy responses of powder and pellet samples. The energy responses of TLD100 for the photon energies of 0.662, 6, 18 MV are matched well inside itself. The ratio of TL signal measured for TLD100 chips to the signal obtained for the powder and pellet LTB:Mn phosphors with the same dose for 6 and 18 MV photon energies are around 30 and 200, respectively.

The powder LTB:Mn 0.04 M % samples were also irradiated with a 220 kV_p x-ray source, with an appropriate build-up material. A dose of 2 Gy was delivered, similar to the photons with the previously employed energies. The two TL glow curves of ~0.040 - 0.080 MV and 0.662 MV photons were compared and agreed well within 1 % deviation with each other regarding the sensitivities (counts/mg) of specimens and subsequent reading of both after the same elapsed time interval.

3.6 Electron energy response

The energy response of powder and pellet LTB:Mn 0.04 M % and TLD100 chips relative to electron energy after a 2 Gy electron dose exposure delivered from a LINAC was demonstrated. The dependence of them to 6, 9, 12 and 15 MeV electron energies were determined. Relatively uniform response was observed for powder and pellet LTB:Mn samples and TLD100 chips. The ratio of minimum and maximum readings quantifies the value of around 1 for each group (powder LTB:Mn samples, pellet LTB:Mn samples and TLD100 chips) in itself. The TL sensitivity shows that the powder LTB:Mn 0.04 M % has almost ~6 times higher sensitivity compared to that of pellet LTB:Mn 0.04 M %. At the dose level of interest, the ratios between the energy independent responses of TLD100 chips to that of powder and pellet LTB:Mn samples were 40 and 250, respectively.

3.7 TL repeatability studies

The dose dependence of the TL curves when the samples are repeatedly annealed and irradiated with the same dose of 1 Gy was obtained. The TL reproducibility of the beta dose was tested using repeated cycles of the same furnace annealing, irradiation and readout. The furnace annealing of 400 ^0C for 30 minutes was performed. The TL sensitivity (glow curve area per unit mass of the dosimeter for those measurements) indicated a very good uniformity over 9 repeated cycles. The deviation from the first readout value was at most -7 % based on standard deviation.

3.8 Decay of stored energy

Fading characteristics of beta irradiated LTB:Mn were checked by storing fresh LTB:Mn 0.04 M% phosphor powder samples for 30 days in the dark and at room temperature with humidity around 46% RH in the laboratory after the exposure of a 1 Gy beta dose. Initially, for lower temperature peak (at ~100 ^{0}C), a very strong fading rate was observed in 3 hours and it was completely faded in 12 hours (Fig. 12). The result of investigations on the decay of stored energy in LTB:Mn 0.04 M% phosphor was determined. For high temperature peak (intense peak, at ~260 ^{0}C) the fading rate was nearly 10% after 1 month. The results of fading of high temperature peak revealed that the fading on the seventh day is 27%, on the fourteenth day it is 10%, on the twenty-first day it is 2%, whereas after 30 days the total fading is again 10%. The maximum fading recorded was on the seventh day after the exposure of the samples. Then instead of fading, a growth of peak height to 10 % over two weeks and another increase to 2 % after three weeks were observed and it showed a forecastable fading when the storage time is elongated (Fig. 13). The initial fall of the TL signal is the result of the escaping of electrons from the shallow traps at room temperature. A sort of recovery due to the growth of the high temperature peak during the following two weeks was observed (perhaps due to a combination of the usual thermal decay and a tunneling transfer among the traps) and fading for longer duration. Typically such abnormal fading curves with a small build-up during the initial part of the otherwise normal decay curve were observed for various phosphors by the other authors in the literature [43,44,45,46,9].

The abnormal residual TL in the irradiated phosphor of LTB:Mn after varied periods of storage at room temperature can be explained by [44] (1) Chemical processes such as hydration of surface regions resulting in destruction of traps: Water can be diffused into LTB:Mn phosphor, water related centers may be formed, which act like electron traps (electrochemical charging effect) (2) a tunneling effect which can be mostly a non-thermal process: The tunneling electrons can exist in newly integrated and enlarged dislocations of the crystal structure and as internal charges be transferred within defects inside the band gap of TL material in the dark, at room temperature. Or the wave lengths of the emitted photons might be out of the recorded emission region of the PM tube during the sharp decay of the fading curve observed. Such an abnormal fading could be explained more precisely by making repeated measurements.

4. Conclusion

In our study, we have accomplished the solution combustion synthesis method to prepare the TL material LTB:Mn 0.04 M % and tested it for its dosimetric properties using the mechanisms of thermoluminescence. We emphasized the TL characteristics focusing on the sensitivity, kinetic parameters, the dose response and the photon and electron energy dependence. We also reported recycling and fading characteristics of studied phosphor. The TL results have revealed very important characteristics such as linear dose response at low doses, up to 10 Gy. Between a 10 – 100 Gy absorbed dose, the dose response curve emerges superlinearity characteristics. Annalakshmi et al. reported a similar result for the dose values up to 10 Gy for photon response of 0.32 wt % Mn doped $Li_2B_4O_7$ [9]. Danilkin et al. studied TL dose dependencies for Mn doped $Li_2B_4O_7$. Two groups of samples studied showed supralinearity at doses from 1-500 Gy [47]. The dose response characteristics of the powder and pellet samples show a perfect parallel increment with dose values up to 100 Gy, and are very interesting, because it shows the possibility of utilizing the dosimeter in either form for absolute

dose determinations with satisfactory reliability. The calculated low photon energy dependence (less than 1 MV), at ~ 40-80 keV and 662 keV, of LTB:Mn was somewhat higher than that of high energy photons. According to the data showing similar LTB:Mn phosphor sensitivity to different electron energies, to evaluate the LTB:Mn material exposed with one electron energy without derivation of any calibration curve at any other electron energy can be used for dose determinations. The main glow peak (without deconvolution) is a broad, stable high temperature peak centered near 260 ^{0}C. Further analysis, using T_m-T_{stop} method, along with IR method and CGCD method revealed that the high temperature glow peak after the exposure of 5 Gy beta dose could be separated into the TL peaks centered at 220, 268 and 292 ^{0}C with parameters as reported in Table 1. Relative sensitivity is about one-thirtieth that for TLD100 for both 6 MV and 18 MV x-rays after 2 Gy dose exposure. Recycling property and low fading of this dosimetric peak were determined for LTB:Mn samples in powder form. Fading of the dosimetric peak at 25 ^{0}C for storage at dark is - 10 % in one month.

This paper described the pellets prepared with the mixture of LTB:Mn and KBr revealed parallel dose response with lower TL sensitivity compared with the powder samples over a certain range 0.1-100 Gy. In the future studies, prior to the applications of binding materials to matrix materials we will carefully optimize the binding material and its radiation resistance for the improvement of TL sensitivity. It has been shown that LTB:Mn 0.04 M % phosphor is a promising material which can be used in dosimetry of ionizing radiations. Particularly, It will be used in clinical therapy dosimetry. In future studies, besides doping with Mn, co-doping the sample with rare-earth and different transition metal ions will be performed to improve the thermoluminescence characteristics of the studied phosphor.

5. Acknowledgement

This research is sponsored by NATO's Emerging Security Challenges Division in the framework of the Science for Peace and Security Programme under the project number SfP984649 and the Cukurova University Rectorate through the Projects FUA-2015-4300 and FEF2014YL3. We gratefully acknowledge NATO and Cukurova University for their financial support. We would like to thank Baskent University Hospital, Radiation Oncology Department for their permission in performing the x-ray photon irradiations and the Transfusion Center for gamma ray irradiations, and acknowledge Assoc. Prof. Dr. Aysen Yilmaz for the XRD results. We appreciate Prof. S. Ubizskii, Dr. Y. Zhydachevskii and Dr. A. Luchechko a lot analyzing spectroscopic measurements. The authors also thanks to Inonu University Scientific Research Projects Directorate (BAP) that also partially funded the project (Project Number: 2015/54).

6. References

[1] J.H. Schulman, R.D. Kirk, E.J. West, Use of lithium borate for thermoluminescence dosimetry, in: Proceedings of the International Conference on Luminescence, 1967.

[2] A.S. Pradhan, Thermoluminescence dosimetry and its applications, Radiat. Prot. Dosim., 1 (3) (1981) 153–167.

[3] B.F. Wall, C.M.H. Driscoll, J.C. Strong, E.S. Fisher, The suitability of different preparations of thermoluminescent lithium borate for medical dosimetry, Phy. Med. Biol., 27 (8) (1982) 1023-1034.
[4] Y.S. Horowitz, D. Yossian, Computerized glow curve deconvolution: Application to thermoluminescence dosimetry, Radiat. Prot. Dosim., 60 (1995) 1-114.
[5] M. Prokic, Advance in lithium borate TLD preparation, Proceedings of the IRPA Regional Congress on Radiation Protection in Central Europe, Budapest, Hungary, 2 (1999) 231–239.
[6] G. Kitis, C. Furetta, M. Prokic, V. Prokic, Kinetic parameters of some tissue equivalent thermoluminescence materials, J. Phys. D. Appl. Phys., 33 (2000) 1252-1262.
[7] M. Ignatovych, V. Holovey, A. Watterich, T. Vidoczy, P. Baranyai, A. Kelemen, V. Ogenko, O. Chuiko, UV and electron radiation-induced luminescence of Cu-and Eu-doped lithium tetraborates, Radiat. Phys. Chem., 67 (2003) 587–591.
[8] D.S. Thakare, S.K. Omanwar, S.V. Moharil, S.M. Dhopte, P.L. Muthal, V.K. Kondawar, Combustion synthesis of borate phosphors, Opt. Mater., 29 (2007) 1731-1735.
[9] O. Annalakshmi, M.T. Jose, G. Amarendra, Dosimetric characteristics of manganese doped lithium tetraborate - an improved TL phosphor. Radiat. Meas., 46 (2011) 669-675.
[10] M. Ignatovych, M. Fasoli, A. Kelemen, Thermoluminescence study of Cu, Ag and Mn doped lithium tetraborate single crystals and glasses, Radiat. Phys. Chem., 81 (2012) 1528-1532.
[11] B.A. Doull, L.C. Oliveira, E.G. Yukihara, Effect of annealing and fuel type on the thermoluminescent properties of $Li_2B_4O_7$ synthesized by Solution Combustion Synthesis, Radiat. Meas., 56 (2013) 167-170.
[12] M. Prokic, Lithium borate solid TL detectors, Radiat Meas., 33 (2001) 393-396.
[13] C. Furetta, M. Prokic, R. Salamon, V. Prokic, G. Kitis, Dosimetric characteristics of tissue equivalent thermoluminescent solid TL detectors based on lithium borate, Nucl. Instrum. Meth. A, 456 (2001) 411-417.
[14] M. Ignatovych, V. Holovey, T. Vidoczy, P. Baranyai, and A. Kelemen., Spectral study on manganese and silver doped lithium tetraborate phosphors, Radiat. Phys. Chem., 76 (2007) 1527-1530.
[15] S.M. Kaczmarek, $Li_2B_4O_7$ glasses doped with Cr, Co, Eu and Dy, Opt. Mater., 19 (1) (2002), 189-194.
[16] S.M. Kaczmarek, T. Tsuboi, G. Boulon, Valency states of Yb, Eu, Dy and Ti ions in $Li_2B_4O_7$ glasses, Opt. Mat., 22 (4) (2003) 303-310.
[17] D. Piwowarska, S.M. Kaczmarek, M. Berkowski, I. Stefaniuk, Growth and EPR and optical properties of $Li_2B_4O_7$ single crystals doped with Co^{2+} ions, J. Cryst. Growth, 291 (2006) 123-129.
[18] E. Pekpak, A. Yılmaz, G. Özbayoglu, The effect of synthesis and doping procedures on thermoluminescent response of lithium tetraborate, J. Alloy. Compd., 509 (2011) 2466–2472.
[19] O. Annalakshmi, M.T. Jose, U. Madhusoodanan, B. Venkatraman, G. Amarendra, Kinetic parameters of lithium tetraborate based TL materials, J. Lumin. 141 (2013) 60–66.
[20] D. Podgórska, S.M. Kaczmarek, W. Drozdowski, M. Wabia, M. Kwaśny, S. Warchoł, V.M. Rizak, Recharging processes of Mn ions in $Li_2B_4O_7$:Mn single crystal and glass under influence of g-irradiation and annealing, Molecul. Phys. Rep., 39 (2004) 199-222.
[21] D. Podgórska, S.M. Kaczmarek, W. Drozdowski, M. Berkowski, A. Worsztynowicz, Growth and optical properties of $Li_2B_4O_7$ single crystals pure and doped with Yb, Co, Eu and Mn ions for nonlinear applications, Acta Phys. Pol. A, 107 (2005) 507-516.

[22] M. Kayhan, A. Yilmaz, Effects of synthesis, doping methods and metal content on thermoluminescence glow curves of lithium tetraborate, J. Alloy. Compd, 509 (30) (2011) 7819–7825.
[23] V. Nagirnyi, E. Aleksanyan, G. Corradi, M. Danilkin, E. Feldbach, M. Kerikmäe, A. Kotlov, A. Lust, K. Polgár, A. Ratas, I. Romet, V. Seeman, Recombination luminescence in $Li_2B_4O_7$ doped with manganese and copper, Radiat. Meas., 56 (2013) 192-195.
[24] W. Drozdowski, K. Brylew, S.M. Kaczmarek, D. Piwowarska, Y. Nakai, T. Tsuboi, W. Huang, Studies on shallow traps in $Li_2B_4O_7$:Eu, Mn, Radiat. Meas., 63 (2014) 26-31
[25] S. Kar, C. Debnath, S. Verma, V.P. Dhamgaye, G.S. Lodha, K.S. Bartwal, Thermoluminescence studies on single crystal, polycrystalline and glass lithium tetraborate samples irradiated by X-rays from Indus-2, Physica B, 456 (2015) 1-4.
[26] O. Annalakshmi, M.T. Jose, U. Madhusoodanan, J. Sridevi, B. Venkatraman, G. Amarendra, A.B. Mandal, Radiation-induced defects in manganese-doped lithium tetraborate phosphor, Radiat. Prot. Dosim., 163 (1) (2015) 14-21.
[27] V.F. Sears, Neutron scattering lengths and cross sections, Neutron News, 3 (3) (1992) 26-37.
[28] Ya.V. Burak, B.V. Padlyak, V.M. Shevel, Neutron induced defects in the lithium tetraborate single crystals. Radiat. Eff. Defect. S., 157 (2002) 1101-1109.
[29] Ya.V. Burak, V.T. Adamiv, I.M. Teslyuk, V.M. Shevel, Optical Absorption of Isotopically Enriched $Li_2B_4O_7$ Crystals Irradiated by Thermal Neutrons. Radiat. Meas., 38 (2004) 681-684.
[30] U.D. Altermatt, I.D. Brown, A real-space computer-based symmetry algebra, Acta Crystallogr., A 43 (1987) 125–130.
[31] B. Umesh, B. Eraiah, H. Nagabhushana, S.C. Sharma, D.V. Sunitha, B.M.Nagabhushana, J.L. Rao, C. Shivakumara, R.P.S. Chakradhar, Structural characterization, thermoluminescence and EPR studies of Nd_2O_3:Co^{2+} nanophosphors. Mater. Res. Bull., 48 (2013) 180–187.
[32] J. Malleshappa, H. Nagabhushana , S.C. Sharma , D.V. Sunitha , N. Dhananjaya , C. Shivakumara , B.M. Nagabhushana, Self propagating combustion synthesis and luminescent properties of nanocrystalline CeO_2:Tb^{3+} (1–10 mol%) phosphors, J. Alloy. Compd, 590 (2014) 131–139.
[33] B.S. Ravikumar, H. Nagabhushana, S.C. Sharma , B.M. Nagabhushan, Low temperature synthesis, structural and dosimetric characterization of $ZnAl_2O_4$:Ce^{3+} nanophosphor, Spectrochim. Acta A., 122 (2014) 489–498.
[34] J. Manam, S.K. Sharma, Determination of trapping parameters from thermally stimulated luminescence glow curves of Mn-doped $Li_2B_4O_7$ phosphor, Radiat. Eff. Defect. S., 163 (10) (2008) 813-819.
[35] S.W.S. McKeever, Thermoluminescence in solids, Cambridge University Press, 1988.
[36] S.W.S. McKeever, On the Analysis of Complex Thermoluminescence Glow-Curves: Resolution into Individual Peaks, Phys. Status Solidi (a), 62 (1980a) 331 – 340.
[37] C. Furetta, Handbook of Thermoluminescence, 2nd revised edition, World Scientific Publishing Co. Pte. Ltd, Singapore, 2010.
[38] C. Furetta, G. Kitis, C.H. Kuo, Kinetics parameters of CVD diamond by computerised glow-curve deconvolution (CGCD), Nucl. Instrum. Meth. B, 160 (1) (2000) 65-72.
[39] R. Chen and Y. Kirsh, The Analysis of Thermally Stimulated Processes, Pergamon Press, Oxford, New-York, 1981.
[40] A.N. Yazici, R. Chen, S. Solak, Z. Yegingil, The Analysis of thermoluminescent glow peaks of CaF_2:Dy (TLD-200) after β-irradiation, J. Phys. D. Appl. Phys., 35 (2002) 2526-2535.
[41] G. Kitis, J.M. Gomez-Ros, J.W.N. Tuyn, Thermoluminescence glow-curve deconvolution functions for first, second and general orders of kinetics. J. Phys. D: Appl. Phys., 31 (1998) 2636–2641.

[42] W.A. Langmead, B.F. Wall, A TLD System based on lithium borate for measurement of doses to patient undergoing medical irradiation. Phy. Med. Biol., 21 (1) (1976) 39-51.
[43] Z. Spurny, and J. Kvasnika, Short-term fading of different thermoluminescent phosphors, In: T. Niewiadomsky, ed. Proceedings Of The Fourth International Conference On Luminescence Dosimetry, Krakow, Poland, Institute of Nuclear Physics, 1 (1974) 255-262.
[44] K.S.V. Nambi, Thermoluminescence: Its understanding and applications, Atomic Energy Agency Publications, Sao Paulo, Brasil, 1977.
[45] C. Furetta, R. Pellegrini, Some dosimetric properties of Li_2O_7:Mn (TLD-800), Radiat. Eff. Defect. S., 58 (1-2) (1981) 17-23.
[46] Y.S. Horowitz, Thermoluminescence and thermoluminescent dosimetry, v1, CRC Press, Boca Raton, FL, 1984.
[47] M. Danilkin, I. Jaek, M. Kerikmäe, A. Lust, H. Mändar, L. Pung, A. Ratas, V. Seeman, S. Klimonsky, V. Kuznetsov, Storage mechanism and OSL-readout possibility of $Li_2B_4O_7$:Mn (TLD-800), Radiat. Meas., 45 (3–6) (2010) 562–565.

Table 1. Kinetic parameters estimated using IR and CGCD methods.

	Activation energy E_a(eV)	Kinetics order (b)	Frequency factor $(s)s^{-1}$	Methods
P1	1.03±0.12	-	-	IR
220°C	0.95±0.01	1.46±0.05	$5.74x10^8$	CGCD
P2	1,22±0.05	-	-	IR
268°C	1.22±0.01	1.78±0.07	$2.32x10^{10}$	CGCD
P3	1,45±0.04	-	-	IR
292°C	1.44±0.01	1.87±0.05	$5.65x10^{11}$	CGCD

Figure Captions

Figure 1. TL responses for various sintering temperatures.

Figure 2. TL responses of 1 Gy beta dose after sintering at 800 ^{0}C for various times.

Figure 3. The characterization of Mn-doped lithium tetraborate (a) powder X-ray diffraction pattern, (b) IR spectrum and (c - d) SEM image.

Figure 4. PL emission spectra of LTB:Mn. From the emission spectra it is observed that LTB:Mn has an emission around 600 nm which is characteristic of Mn.

Figure 5. Photoluminescence excitation (PL) monitored at the typical emission wavelength of the material (600 nm). Peak of 409 nm in the PLE spectra represents absorption line of LTB:Mn.

Figure 6. Comparison between the TL glow curves for $Li_2B_4O_7$:Mn powder and pellet samples following an exposure of 2 Gy dose. The relative sensitivity of $Li_2B_4O_7$:Mn powder phosphor to beta dose per unit mass compared with that of $Li_2B_4O_7$:Mn pellet phosphor is 4.5 with respect to the total glow curve area integrated (counts).

Figure 7. T_m plotted against to T_{stop} after T_m -T_{stop} procedure from 160 ^{0}C to 320 ^{0}C.

Figure 8. Activation energy (E_a) obtained using RIR method after T_m -T_{stop} procedure from 160 ^{0}C to 320 ^{0}C.

Figure 9. A typical analyzed glow curve LTB:Mn measured after 5 Gy irradiation at RT. The glow curve was measured immediately after irradiation of the sample at a heating rate of 2 ^{0}C/s. Preheating was 160 ^{0}C for 10 s.

Figure 10. The integrated TL glow curve area versus to exposed dose of beta-rays irradiated LTB:Mn 0.04 M % powder and pellet phosphors with varying dosages from 0.1 Gy to 100 Gy.

Figure 11. Dose response (total counts in area integrated/mg) of powder and pellet $Li_2B_4O_7$:Mn 0.04 M % phosphors, and TLD100 chips exposed to beta irradiation 0.1 Gy to 10 Gy from ^{90}Sr/ ^{90}Y source. Lines indicate linearity behavior through 10 Gy data points.

Figure 12. Glow curves for LTB:Mn samples at 30 min, 1 h, 3 h, 6 h, 12 h, 7 d, 14 d, 21 d and 30 d after being irradiated with 1 Gy absorbed dose of beta-rays.

Figure 13. Residual TL of the high temperature peak between temperature 160 and 450 ^{0}C in the irradiated phosphor, put in the drawer, after different periods of storage at room temperature.

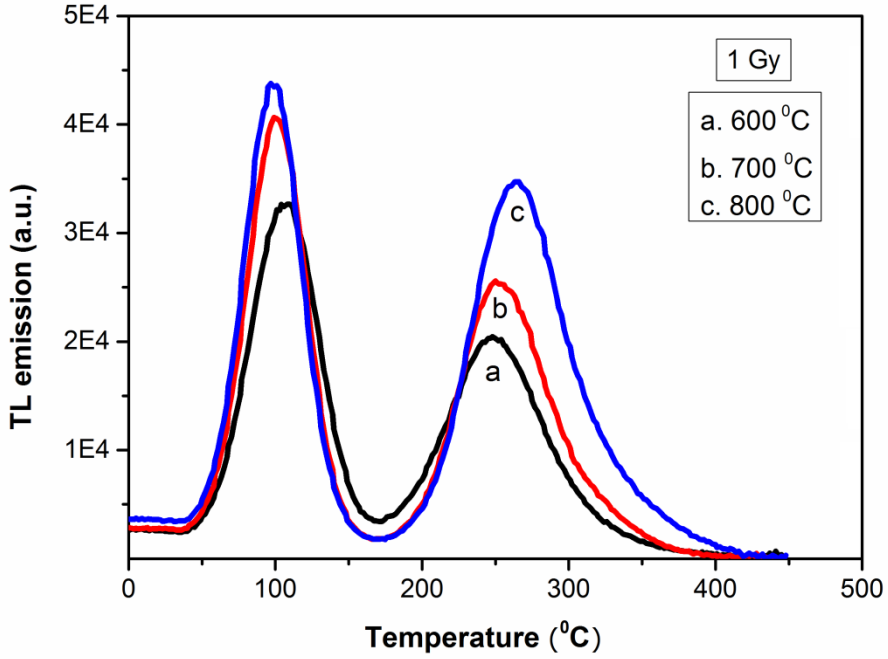

Figure 1

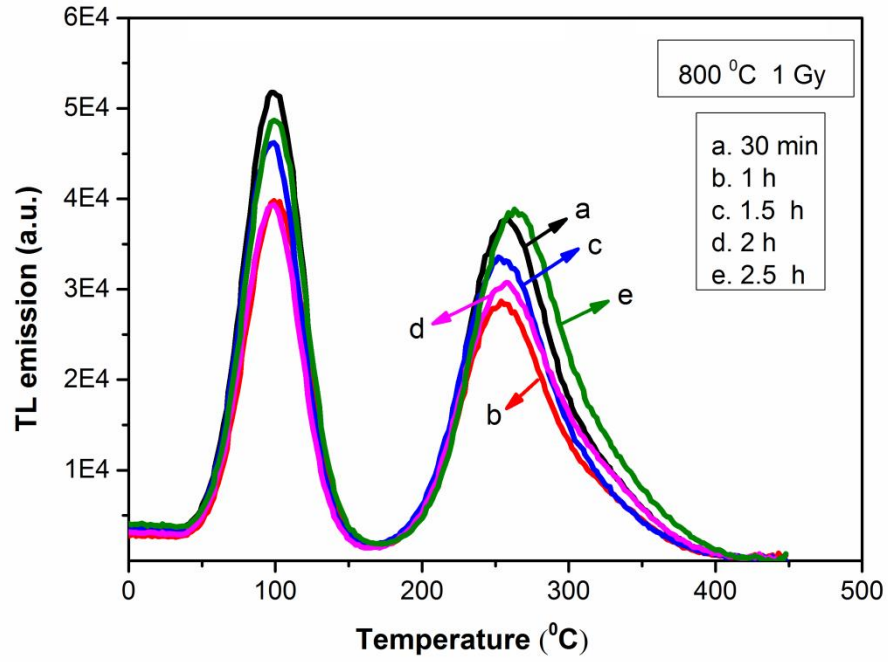

Figure 2

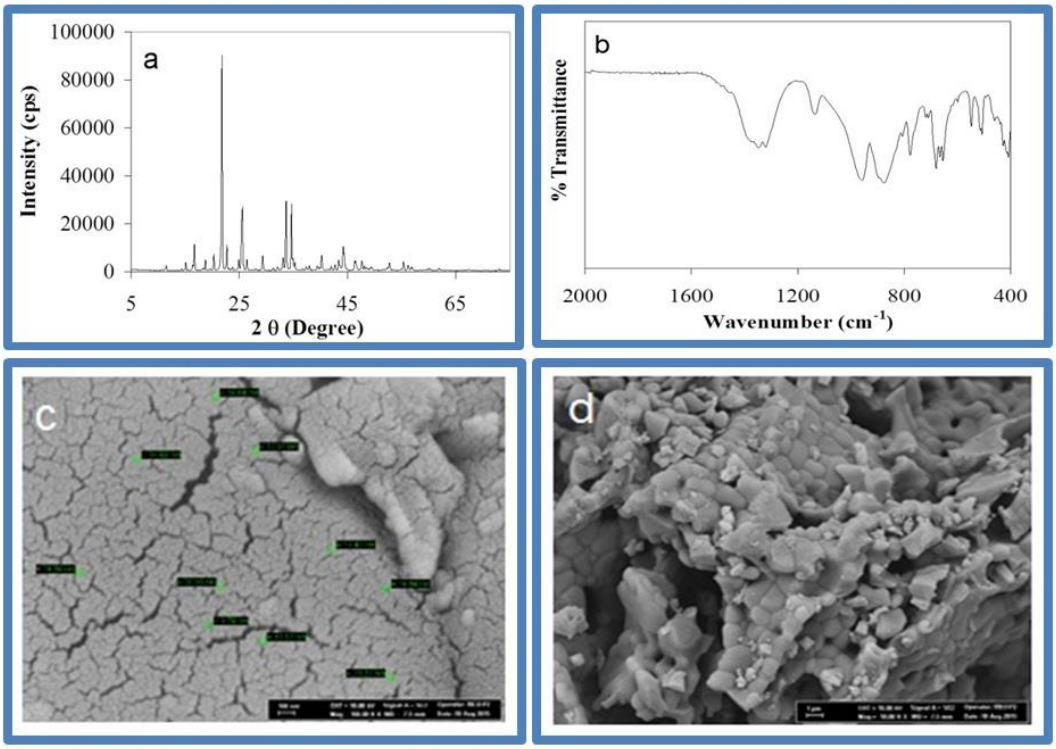
a
Intensity (cps)
100000
80000
60000
40000
20000
0
5
25
45
65
2 θ (Degree)
b
% Transmittance
2000
1600
1200
800
400
Wavenumber (cm-1)
c
d

Figure 3

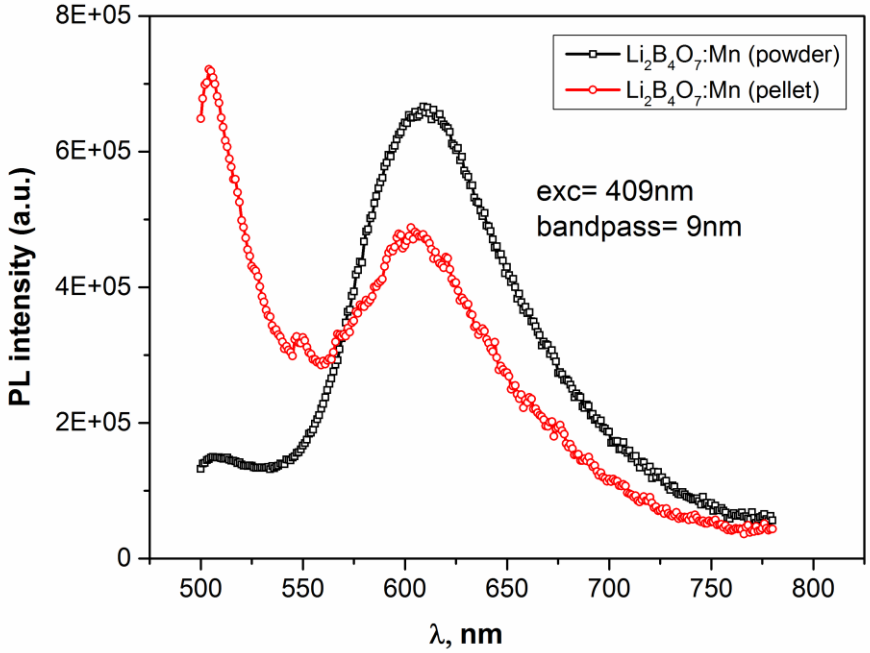

Figure 4

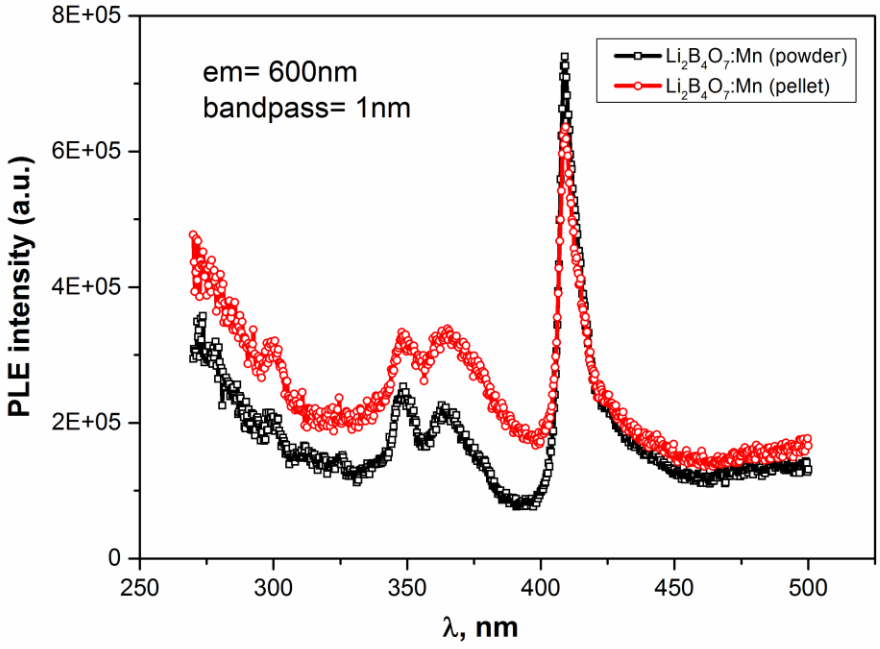

Figure 5

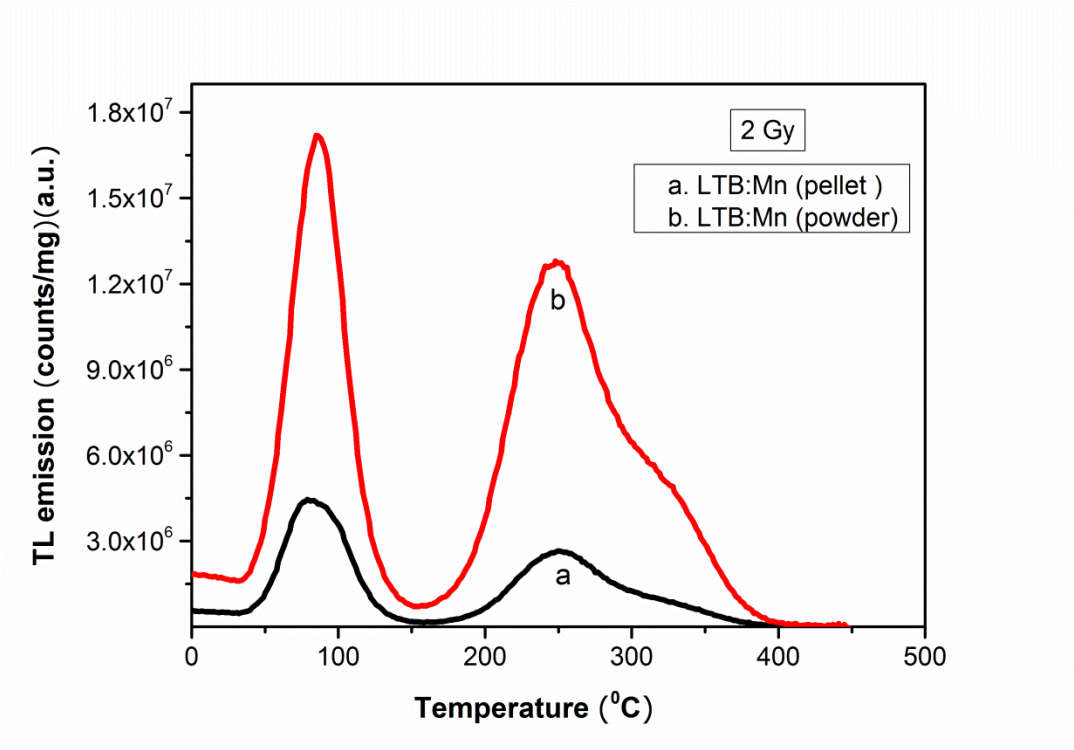

Figure 6

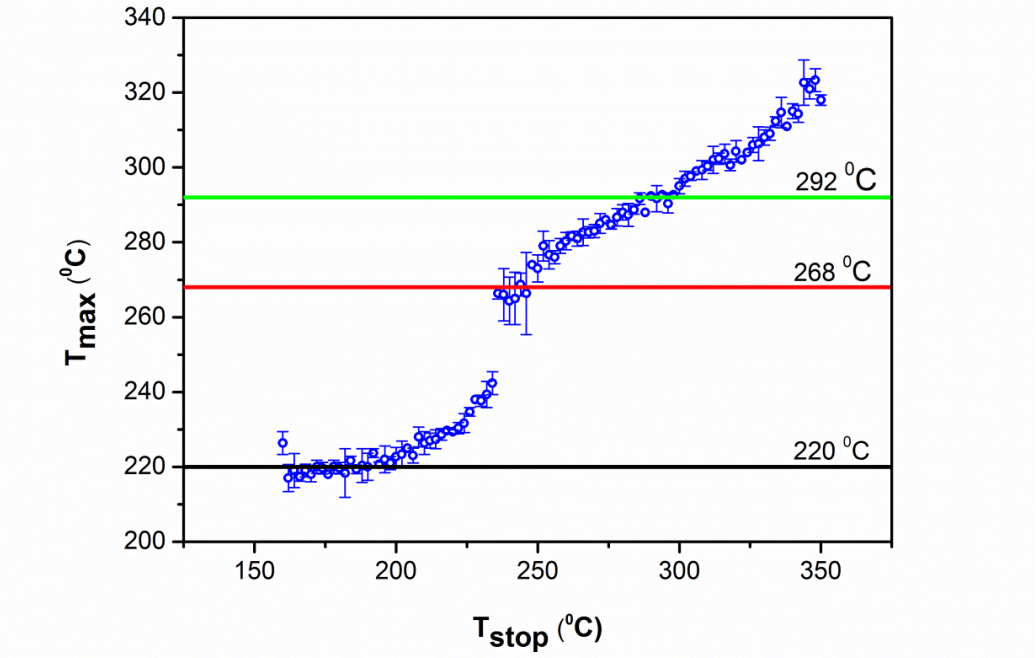

Figure 7

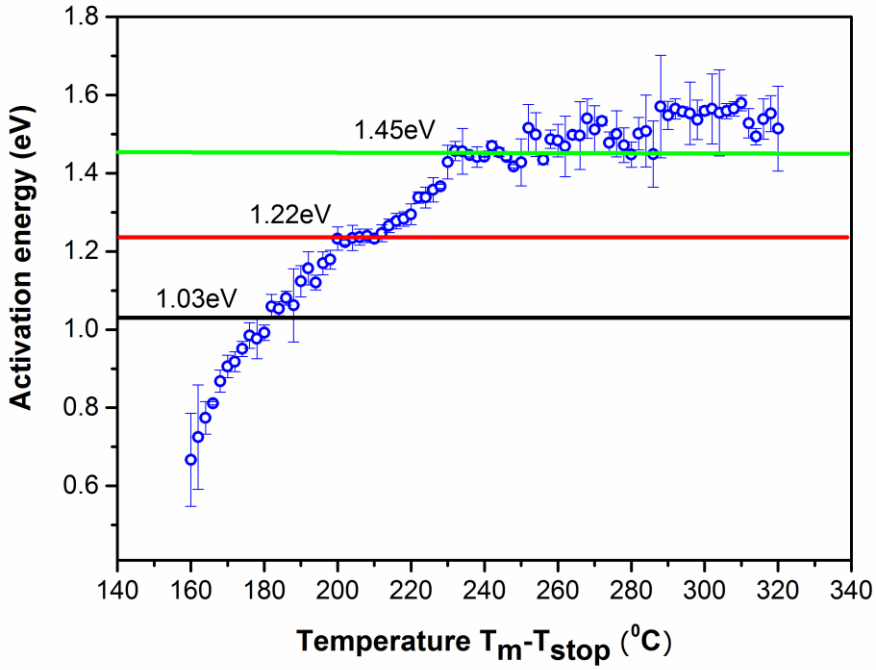

Figure 8

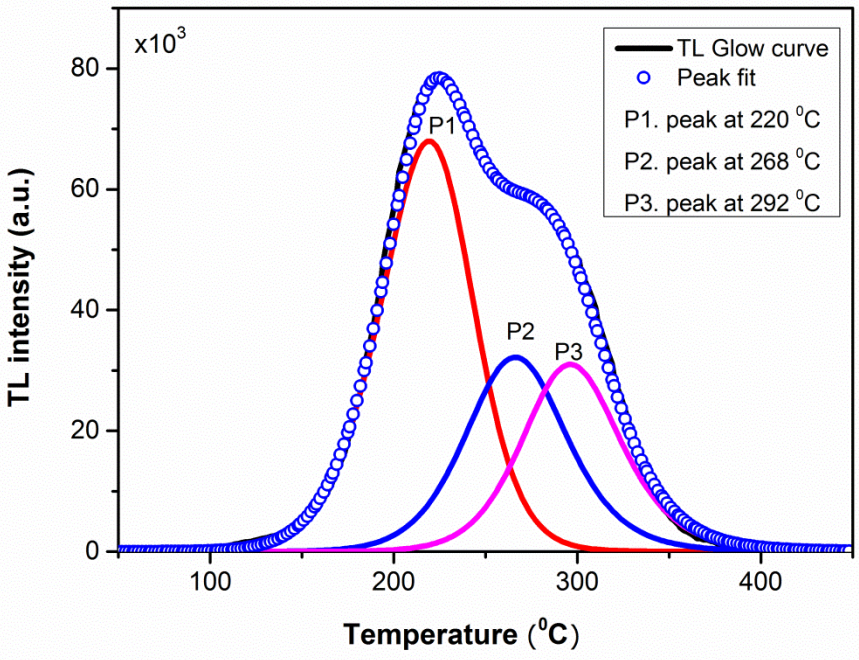

Figure 9

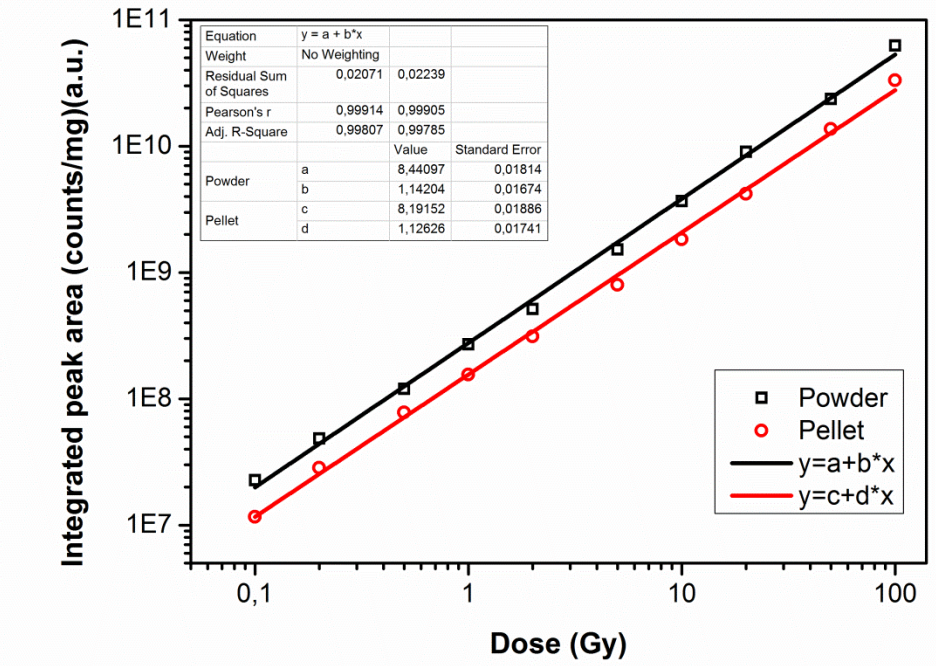

Figure 10

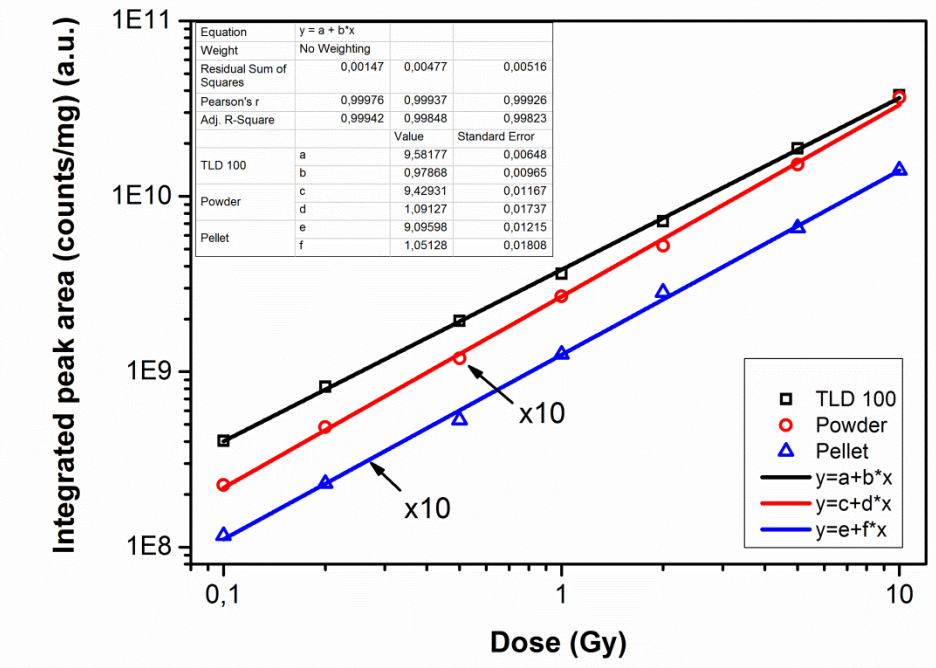

Figure 11

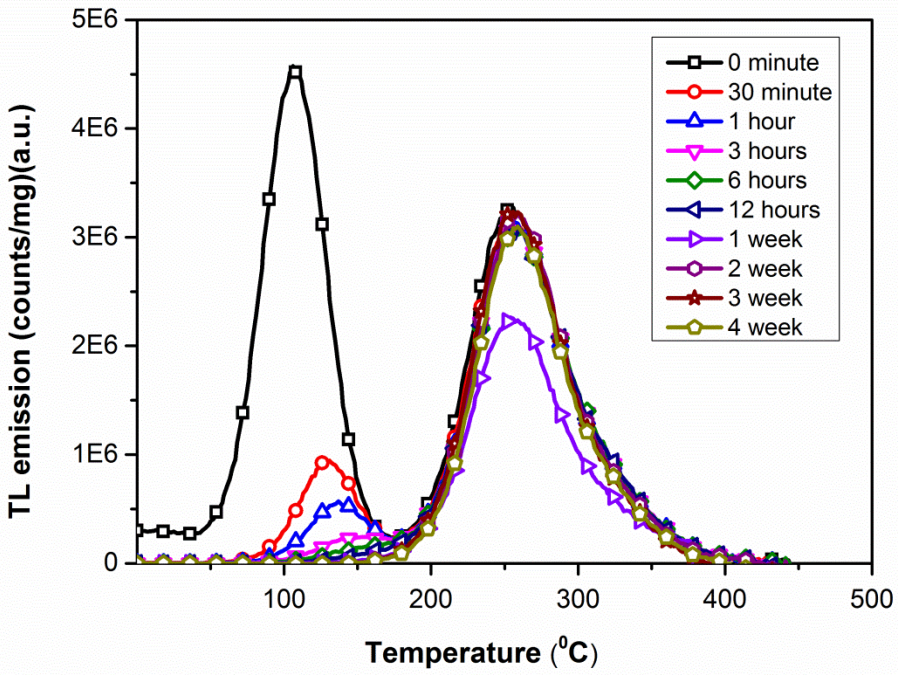

Figure 12

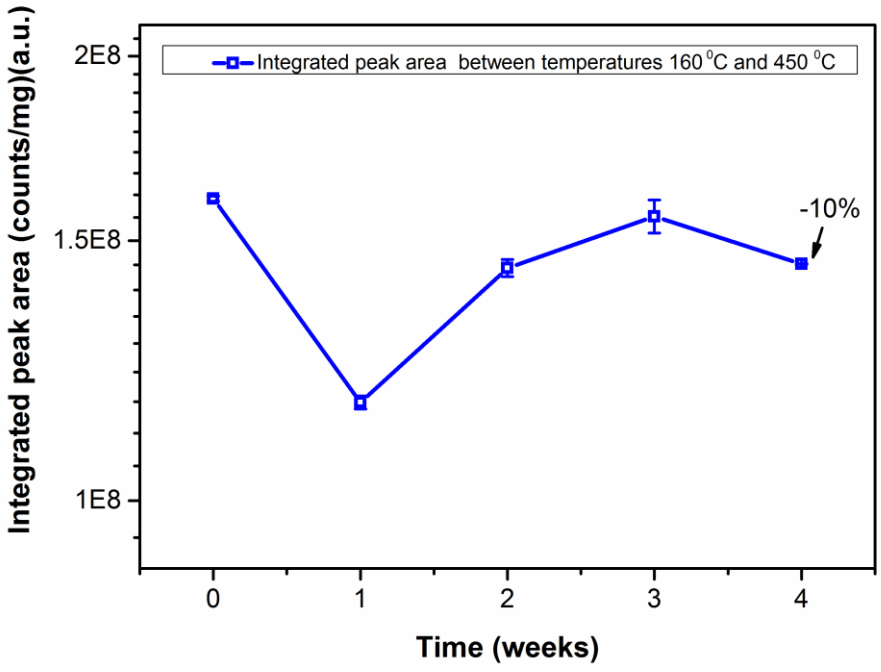

Figure 13